

Electronic Supplementary Information

## Tuning bimetallic catalysts for a selective growth of SWCNTs

Salomé Forel,<sup>a</sup> Alice Castan,<sup>b,c</sup> Hakim Amara,<sup>b</sup> Ileana Florea,<sup>a</sup> Frédéric Fossard,<sup>b</sup> Laure Catala,<sup>c</sup> Christophe Bichara,<sup>d</sup> Talal Mallah,<sup>c</sup> Vincent Huc,<sup>c</sup> Annick Loiseau,<sup>b</sup> and Costel-Sorin Cojocaru<sup>a</sup>

### 1 Size distributions of catalyst nanoparticles

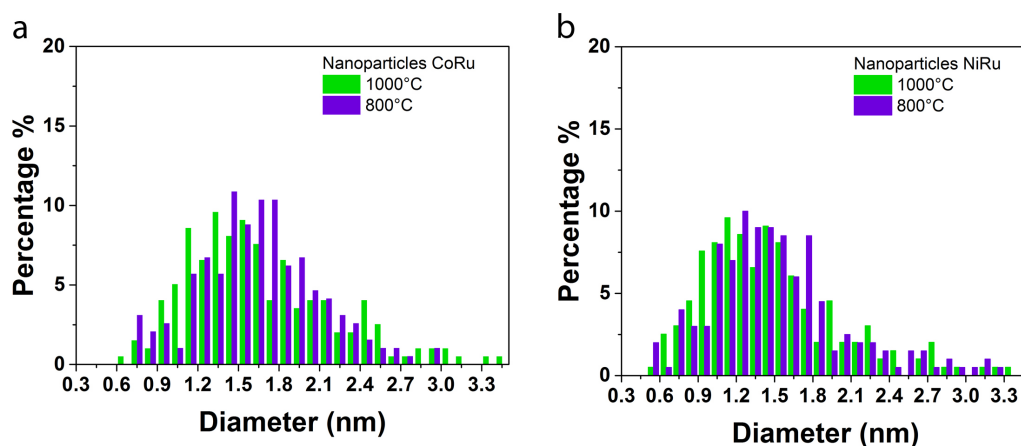


Figure S1: Size distributions of NiRu and CoRu nanoparticles after pretreatment at 800 and 1000°C.

<sup>a</sup> Laboratoire de Physique des Interfaces et des Couches Minces, CNRS, Ecole Polytechnique, 91128, Palaiseau Cedex, France ; E-mail: salome.forel@polytechnique.edu

<sup>b</sup> Laboratoire d'Etude des Microstructures, ONERA-CNRS, UMR104, Université Paris-Saclay, BP 72, 92322 Chatillon Cedex, France ; E-mail: alice.castan@onera.fr, hakim.amara@onera.fr

<sup>c</sup> Institut de Chimie Moléculaire et des Matériaux d'Orsay, CNRS, Université Paris-Sud/Paris Saclay, 15 rue Georges Clemenceau, Orsay, France

<sup>d</sup> Aix Marseille Université, CNRS, Centre Interdisciplinaire de Nanoscience de Marseille, Campus de Luminy, Case 913, F-13288, Marseille, France

## 2 STEM-EDX study of catalyst nanoparticles

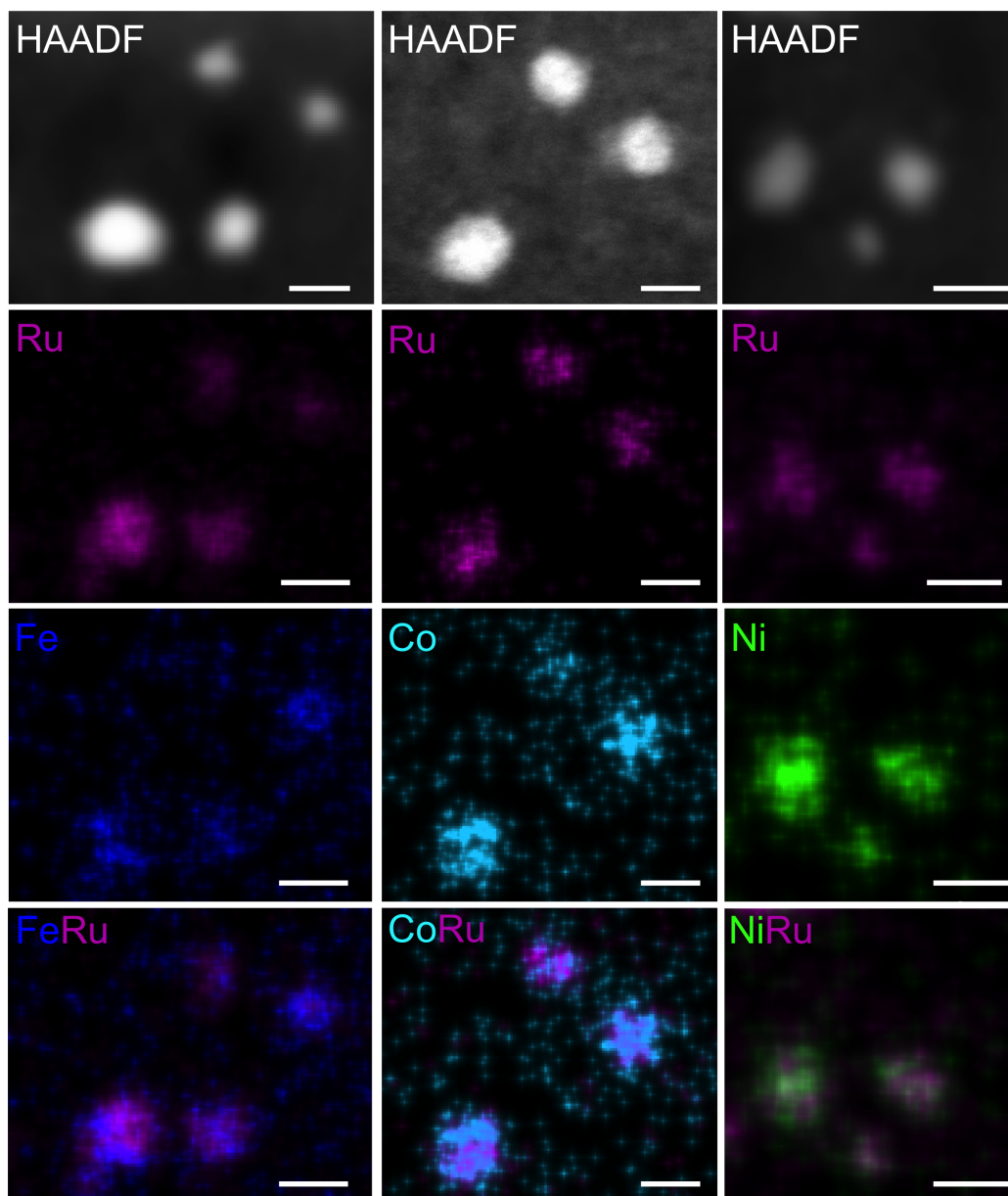


Figure S2: From top to bottom: High annular dark field scanning TEM (HAADF-STEM) images, and STEM energy dispersive X-ray spectroscopy (STEM-EDX) chemical maps for the three catalyst systems (FeRu, CoRu, NiRu). For each image the scale bar is 3 nm.

A more detailed description of the catalyst and catalyst precursor syntheses and characterizations are available in ref<sup>1</sup>. The atomic structures, morphology and composition of the Prussian blue analogs used as catalyst precursors have been determined by infrared spectroscopy, X-ray powder diffraction, TEM and SEM-EDX, demonstrating that small nanoparticles, in cubic face centered structure and with an atomic composition of Fe/Ni/Co:Ru = 1:1 have been obtained. The effective catalyst nanoparticles are obtained through the pyrolysis of PBA nanoparticles, and as we showed that diffusion of metals on the surface is very limited during the catalyst formation process, and that the STEM-EDX study (figure S2) shows that no phase segregation occurs, the catalyst nanoparticles can be expected to be close to 1:1 in metallic ratio, as the precatalysts.

### 3 Methodology

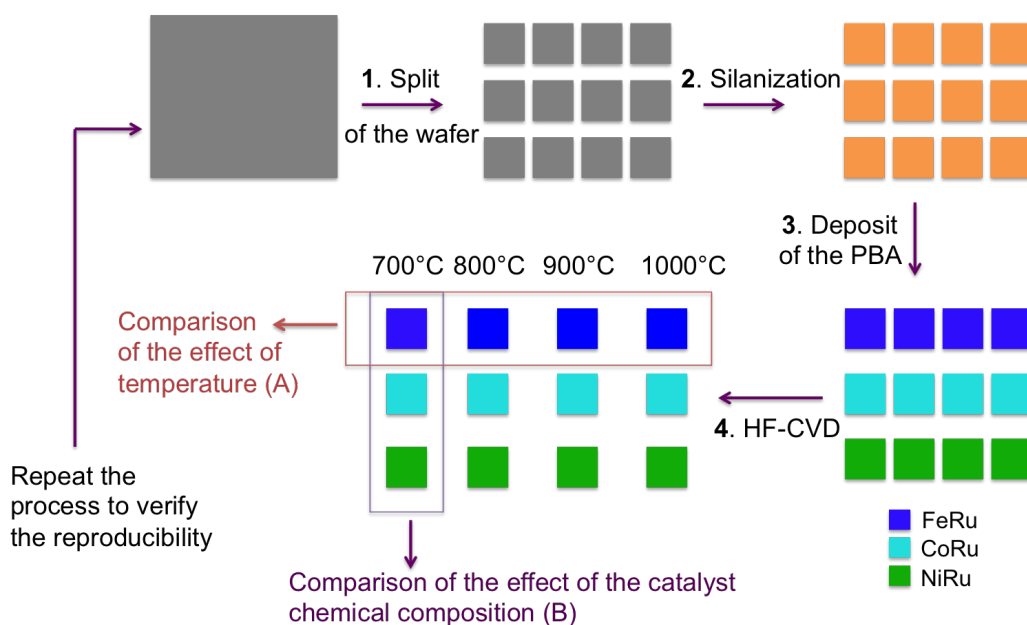


Figure S3: Schematic view of the synthesis process implemented in order to perform a parametric study.

The SWCNT growth process (including pretreatment and growth) is performed in the d-HFCVD at 700°C, 800°C, 900°C, and 1000°C. For each synthesis temperature, the synthesis of SWCNTs is performed on three samples (one of each catalyst) at the same time. Under this condition, we can analyze the effect of the synthesis temperature on the SWCNT structure for a given catalyst (step A), or the effect of the catalyst chemical composition for a fixed growth temperature (step B).

## 4 Yield

SEM images can be used to give some indication of the cover rate over the sample and show that our syntheses present an acceptable yield. Examples of SEM images in the case of SWCNTs grown from FeRu for all the studied temperatures are shown in Fig. S4. Similar results are obtained for the CoRu and NiRu systems.

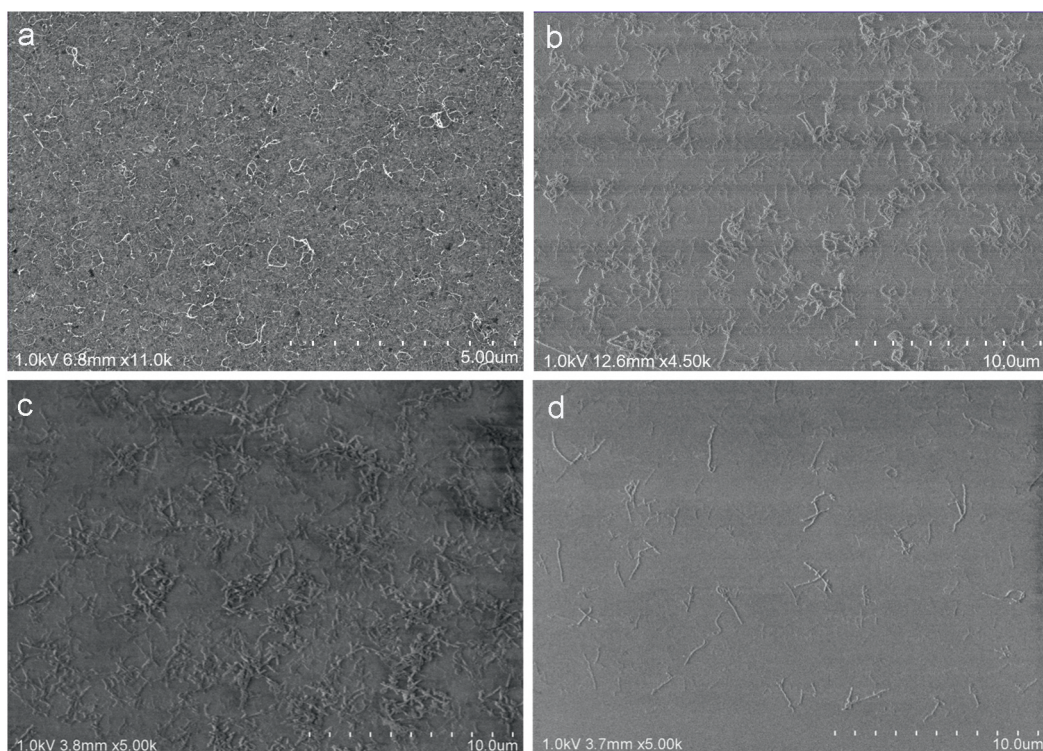


Figure S4: Typical SEM images of SWCNTs grown from the FeRu catalyst at (a) 700°C, (b) 800°C, (c) 900 °C, and (d) 1000 °C. In each image, the substrate appears to be covered by SWCNTs, with a seemingly higher yield for growths at temperatures lower than 1000 °C.

## 5 Reproducibility

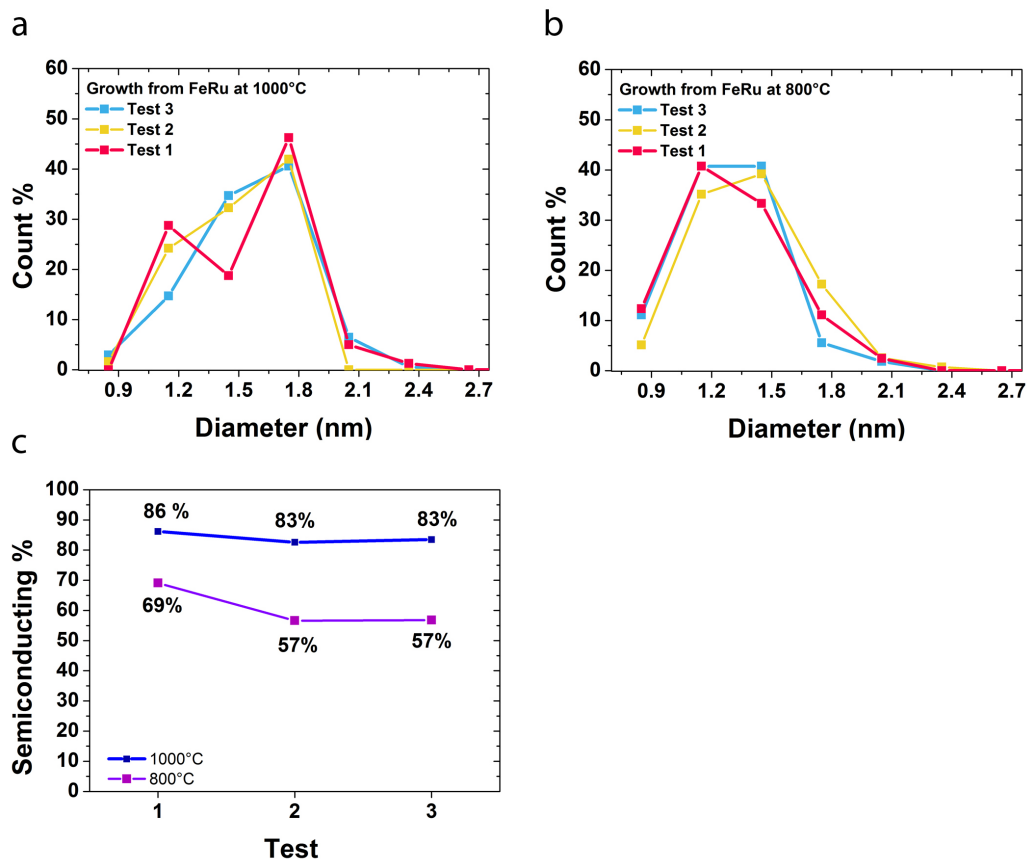


Figure S5: SWCNT diameter distributions obtained from the FeRu catalyst for three different syntheses at (a) 1000°C, and (b) 800°C. (c) Percentage of semiconducting nanotubes obtained for three different syntheses at 800 and 1000°C. Here, the diameter distribution was obtained through statistical Raman spectroscopy analysis with three wavelengths (532 nm, 633 nm, 473 nm).

## 6 Typical TEM images of the SWCNTs

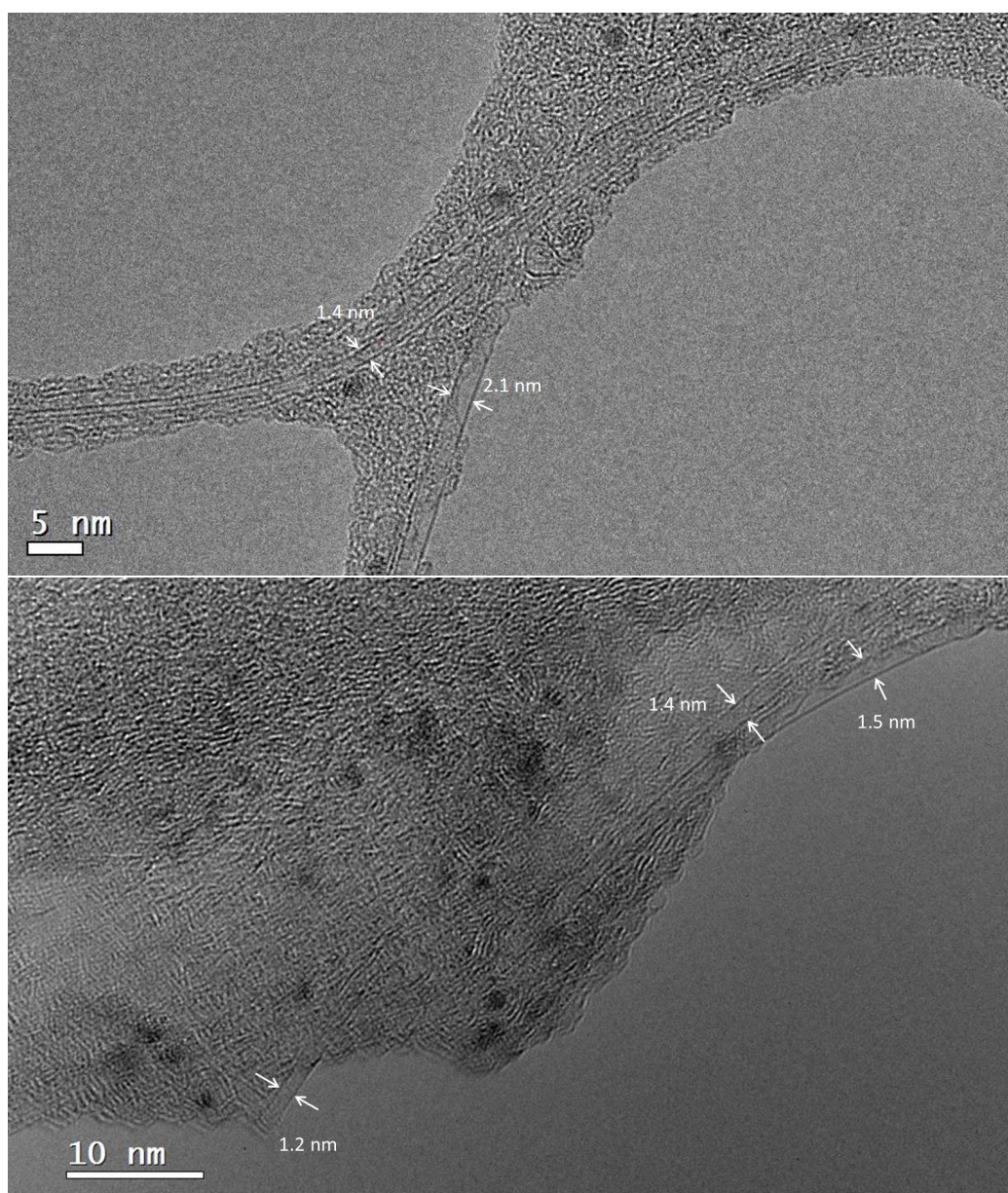


Figure S6: TEM images of SWCNTs for syntheses at 800°C from the FeRu catalyst (top), and the NiRu catalyst (bottom).

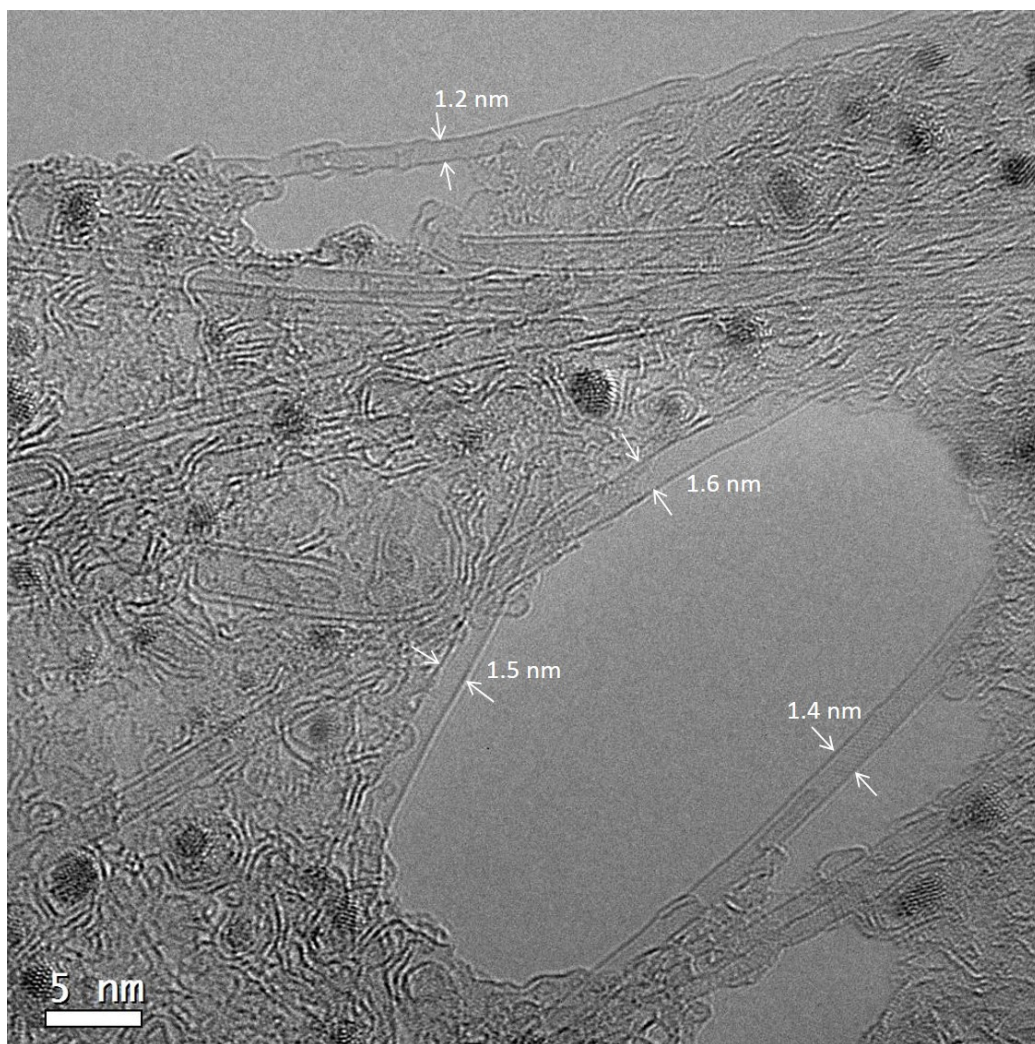


Figure S7: TEM image of SWCNTs for a synthesis at 800°C from the CoRu catalyst



## 7 $D_{NP}/D_{tube}$

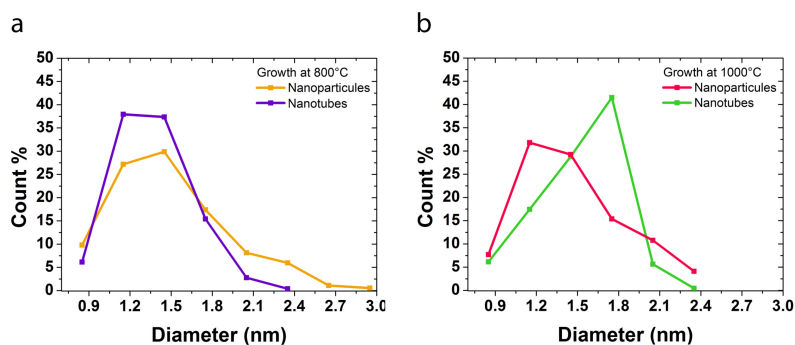


Figure S8: Superimposed diameter distributions of FeRu catalyst nanoparticles and as-grown SWCNTs (based on Raman spectroscopy) for syntheses at (a) 800°C, and (b) 1000°C.

## 8 Bi-temperature synthesis

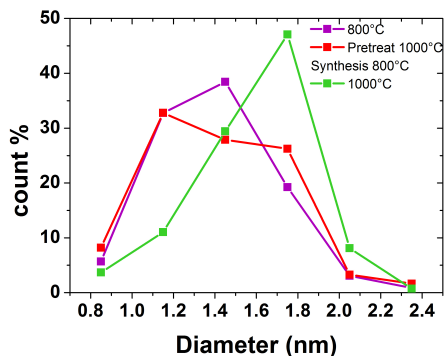


Figure S9: Size distributions of nanotubes grown from the FeRu catalyst for growths at 800°C (pretreatment + growth) (purple line), 800°C with a pretreatment at 1000°C (red line), and at 1000°C (pretreatment + growth) (green line). Here, the diameter distributions were obtained through statistical Raman spectroscopy analysis with three wavelengths (532 nm, 633 nm, 473 nm).

## 9 SWCNT-FETs

### 9.1 Geometry

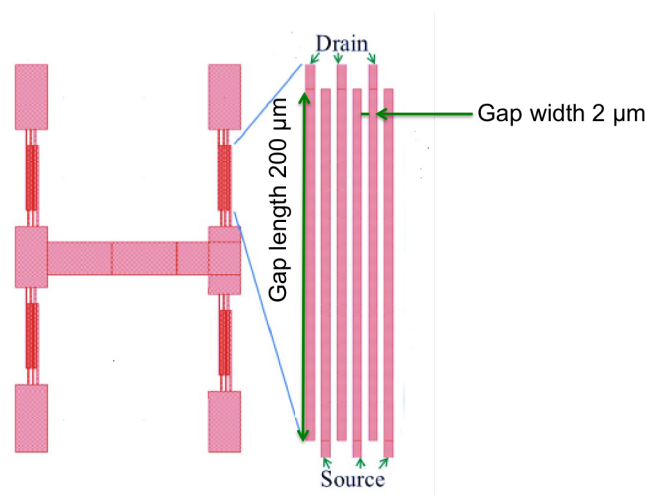
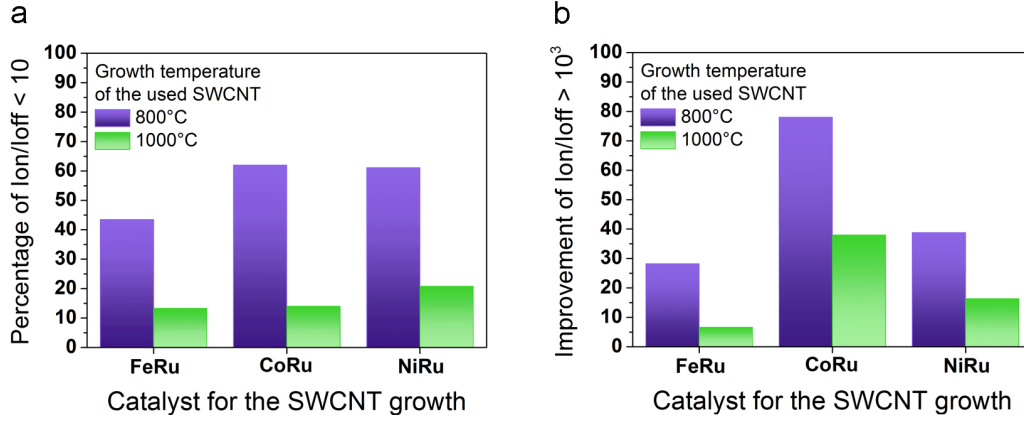


Figure S10: Schematic view of the transistor geometry.

### 9.2 Characterization

We check that an increased presence of amorphous carbon present over the wafers' surface for synthesis at low temperature is not responsible for the higher percentage of ineffective transistor. In Raman spectroscopy, presence of amorphous carbon can be detected through the so-called D-band around  $1350\text{ cm}^{-1}$ . Gao and co-worker, showed that for isolated SWCNTs, the full width half maximum (FWHM) is between  $20\text{ cm}^{-1}$  up to  $40\text{ cm}^{-1}$  for an excitation at  $632\text{ nm}^2$ . Picher and co-worker<sup>3</sup>, for an excitation at  $532\text{ nm}$ , reported a FWHM D-band between  $50\text{-}60\text{ cm}^{-1}$  for CVD SWCNTs comparable with the FWHM D-band of HiPco nanotubes in the same condition (FWMH  $45\text{ cm}^{-1}$ ). On the contrary they found a D-band FWHM in the range of  $130\text{-}190\text{ cm}^{-1}$  for amorphous carbon. In our synthesis, the full-

width half-maximum of the D-band is found between 60-80  $cm^{-1}$  and no significant difference in the FWHM is observed for the different synthesis temperature for any of the studied catalysts (see table in Figure S11).



catalyst	growth temperature	FWMH (excitation at 532nm)
FeRu	800 °C	72.6 ± 2.4
	1000 °C	79.9 ± 2.2
CoRu	800 °C	59.8 ± 2.5
	1000 C	63.9 ± 5.1
NiRu	800 °C	71.4 ± 0.98
	1000 °C	72.4 ± 2.66

Figure S11: (a) Percentage of transistors presenting an Ion/Ioff ratio inferior to 10 for integrated SWCNTs grown from each catalyst at 800 and 1000 °C (before electrical breakdown). (b) Percentage of transistors presenting an improvement of their Ion/Ioff ratio superior to 10<sup>3</sup> after electrical breakdown for integrated SWCNT grown from each catalyst at 800 and 1000 °C **Table** Table of the FWHM of the Raman D-band of samples grown from each catalyst at 800 or 1000 °C.

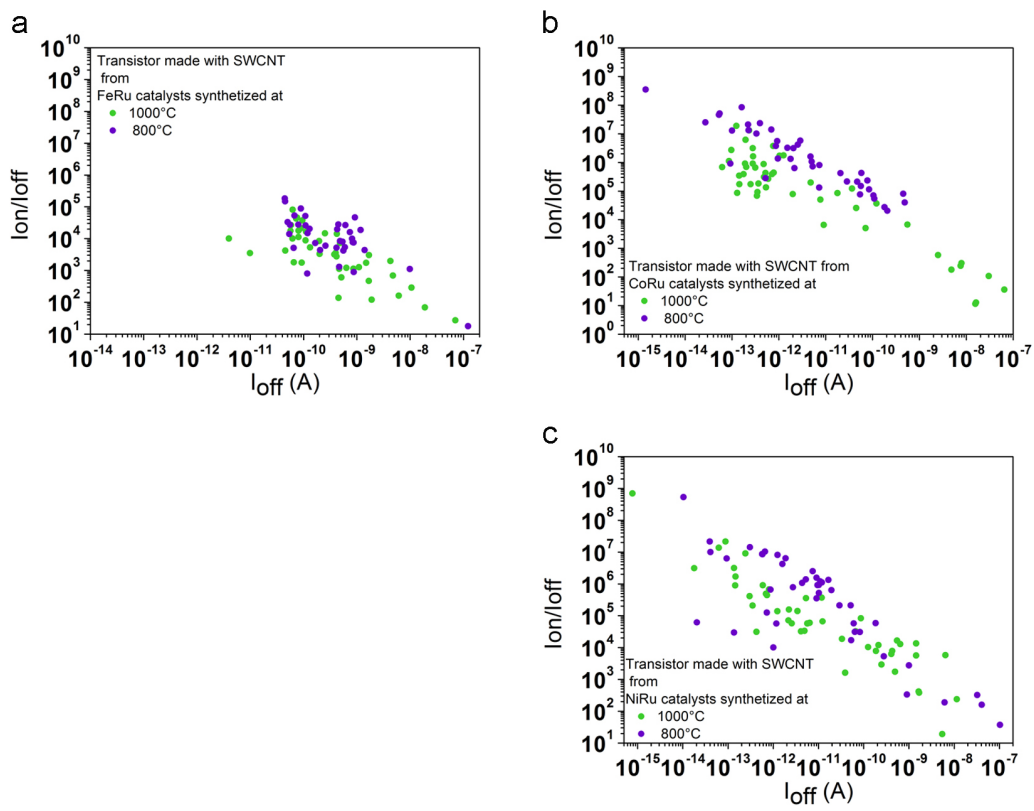


Figure S12:  $I_{on}/I_{off}$  ratio versus  $I_{off}$  of FET-device after electrical breakdown fabricated from a FeRu catalyst b CoRu catalyst c NiRu catalyst

## References

- [1] A. Castan, S. Forel, L. Catala, I. Florea, F. Fossard, F. Bouanis, A. Andrieux-Ledier, S. Mazerat, T. Mallah, V. Huc, A. Loiseau and C. Cojocaru, *Carbon*, 2017, **123**, 583 – 592.
- [2] B. Gao, Y. Zhang, J. Zhang, J. Kong and Z. Liu, *The Journal of Physical Chemistry C*, 2008, **112**, 8319–8323.
- [3] M. Picher, E. Anglaret, R. Arenal and V. Jourdain, *Nano Lett.*, 2009, **9**, 542–547.